Future Technology
Open Access Journal
ISSN 2832-0379

August 2026| Volume 05 | Issue 03 | Pages 57-68

Journal homepage: https://fupubco.com/futech

https://doi.org/10.55670/fpll.futech.5.3.5

Future Publishing LLC

Article

Design and fabrication of an efficient solar powered desalination system for remote communities

Sujesh Kumar[1]*, G.C. Prabhakar[2], Sandhyarani Mahalik[3], Sandeep Kumar Sahoo[4], Prashant Kharote[5], Abdul Khadar Asundi[6], Mohammed Hameeduddin Haqqani[7]

[1]Department Of Aeronautical Engineering, Mangalore Institute of Technology and Engineering, Badaga Mijar, India
[2]EEE Department, VNR Vignana Jyothi Institute of Engineering and Technology, Hyderabad
[3]Department of Computer Science Engineering and Applications Indira Gandhi Institute of Technology, Sarang, Odisha, India
[4]Department of Metallurgical and Materials Engineering, Indira Gandhi Institute of Technology, Sarang, Odisha, India
[5]Department of Electronics and Telecommunication Engineering, Mukesh Patel School of Technology Management & Engineering, Narsee Monjee Institute of Management Studies (NMIMS) Deemed-to-University, Mumbai, India
[6]Electrical and Electronics Engineering, Electrical Power System, Ballari Institute of Technology and Management, Ballari, Karnataka, India
[7]Mechanical Engineering, Career Point University, Kota, Rajasthan, India

ARTICLE INFO

Article history:
Received 15 November 2025
Received in revised form
10 March 2026
Accepted 22 April 2026

Keywords:
Solar-powered desalination, Off-grid systems, Reverse osmosis, Renewable energy integration

*Corresponding author
Email address:
sujesh@mite.ac.in

DOI: 10.55670/fpll.futech.5.3.5

ABSTRACT

Solar desalination is a viable solution to freshwater scarcity in remote, off-grid communities without centralized infrastructure. In this work, the design, performance, and evaluation of an autonomous photovoltaic (PV)-battery-reverse osmosis (RO)-water tank desalination system are presented using simulation. The system is modeled in MATLAB software at an hourly resolution for one complete year (8760h) with realistic climatic data from the POWER (Power System Energy) database at the National Aeronautics and Space Administration. Physically consistent models are applied to PV generation, battery energy-power behavior, RO-specific energy consumption, and freshwater storage dynamics. Baseline results indicate that a community demand of 10 m^3/day can be met with 98.63% daily reliability, resulting in 3643.73 m^3/year of desalinated water and 0.319% unmet demand, with a realized SEC of 4.74 kWh/m^3. However, only 56.43% of the available PV-bus energy is utilized, indicating considerable PV curtailment. The outcome of phase 2 indicates that a decrease in the levelized cost of water (LCOW) through relaxing reliability to 95% daily, without compromising acceptable service levels, is possible. Demand sensitivity, design space exploration, and dispatch policy comparison reveal the great potential of curtailment-aware operation, in conjunction with sufficient water storage, to enhance system efficiency and economic performance in remote desalination applications.

1. Introduction

Freshwater scarcity is one of the most important challenges that the world faces globally and the consequences are particularly dire in remote and off-grid communities where centralised water infrastructure, reliable electricity and logistical access are limited. In such areas, poor access to safe drinking water limits health, livelihood and socioeconomic development. Climate change, population growth and the growing demand for water are further factors that put added pressure on these systems, further boosting the need for decentralized, robust and sustainable solutions to water supply. Desalination provides a viable pathway for the increase of freshwater availability in water stressed coastal and arid regions where saline or brackish water resources are abundant. Traditional desalination in isolated locations has used a standard of diesel generators or grid power. Although technically workable, these options have high operating costs, vulnerability of fuel supply, greenhouse gas emissions and a complexity in maintenance, making it difficult to sustain long term. These limitations have led to the development of increasing interest in renewable-energy powered desalination systems that can be automated and

meet decarbonization goals [1]. Amongst renewable possibilities, solar photovoltaic (PV) reverse osmosis (RO) has emerged as one of the most scalable and extensively studied configurations as RO has comparatively low specific energy consumption, modularity and compatibility with a variable solar input [2]. Advancements in PV, power electronics and stand-alone DC systems as well as solar-coupled RO operation have further increased its suitability for decentralized deployment [3]. Nevertheless, one of the primary challenges is solar intermittency, in particular, situations when the system is forced to satisfy the daily demand of water with no help of grid.

Abbreviations

PV	Photovoltaic
RO	ReverseOsmosis
SEC	Specific Energy Consumption (kWh/m^3)
LCOW	Levelized Cost of Water (USD/m^3)
SOC	State of Charge
GHI	Global Horizontal Irradiance (W/m^2)
NOCT	Nominal Operating Cell Temperature (°C)
OPEX	Operating Expenditure
CAPEX	Capital Expenditure
C-rate	Battery Charge/Discharge Rate (h^{-1})
LCOE	Levelized Cost of Energy
RE	Renewable Energy
SWRO	Seawater Reverse Osmosis
BESS	Battery Energy Storage System

Both electrical and water storages are important in bridging the gap between timing mismatch between solar availability and freshwater needs. Batteries will be able to buffer short term variations in PV, and the freshwater tanks will decouple the water production and consumption and enhance service continuity. However, simplified representations of storage are still widely used in the literature, and misunderstands battery energy capacity and power capability or ignores charge/discharge limiting behavior, both of which can misrepresent the trade-off between reliability and cost of storage system [4]. The PV curtailment is also under-quantified and operational control is often simplified although it is important to quantify its efficiency and cost [5]. More generally integrated renewable-desalination studies do not typically couple issues of reliability, storage sizing, and the hourly nature of the system behavior in physically consistent way [6]. The given research will fill this gap by creating an off-grid PV-battery-RO-water tank desalination framework with explicit curtailment, C-rate constrained battery modeling, and rule-based dispatch analysis [7]. In addition, there is a sensitivity of solar driven RO performance to thermal and operational conditions, which supports the need for realistic system level treatment instead of idealized averaging [8]. The specific objectives of this study are to:

- Develop a physically consistent, hourly time-stepped simulation model of: - an off-grid PV-battery-RO-water tank desalination system that is appropriate for a remote community.
- Quantify the trade-offs between the reliability, the use of solar energy and the levelized cost of water by exploiting the design space through systematic design and dispatch policy analysis.
- Providing design relevant insights supporting efficient sizing and operational strategies - Providing efficient design methods for sizing and designing autonomous solar-powered desalination systems.

2. Literature review

Solar-driven desalination has not ceased to garner interest as a solution to freshwater scarcity in areas that lack constant centralized water and energy infrastructure. Photovoltaic-powered reverse osmosis (PV-RO) is one of the most feasible and the most researched among the renewable-based desalination alternatives due to its comparatively low specific energy usage, modularity and decentralized implementation. The PV-RO technical feasibility in off-grid and weak grid situations, especially in small and medium-scale applications applicable to remote communities, has been established by previous researchers [9]. One of it is the ability to operate reliably when the solar irradiance or water demand vary. Due to the intermittent nature of solar availability, there are temporal mismatches between the availability of energy, desalination production, and water demand. Many studies strive for high reliability through oversizing of PV or the addition of extra storage, both of which add cost [10]. However, reliability has generally been disregarded as it is implicit in that annual water output or average output has been reported without necessarily quantifying unmet demand or service continuity on hourly or daily basis.

Battery storage is frequently put forward to smooth out solar variability, but modeling of battery storage in it is usually simplified. Infineon Power provides a bottom-up approach that highlights the distinction between battery energy capacity (kWh) and power capability (kW) in combination with weak enforcement of the SOC to produce unrealistic long-term behavior and obscure cost-reliability trade-offs [11]. In contrast, freshwater storage tanks have received attention as less expensive forms of buffer, which can decouple production from consumption and can potentially replace electrical storage to some extent with underexplored [12,13]. Operational control is another area that is weakly developed. Common strategies like PV-only or storage priority operation are easy to put in place but potentially do not make good use of surplus solar energy. PV curtailment may be substantial in off-grid applications but is not typically explicitly quantified or even considered as a design objective [14]. Likewise, though LCOW is widely used in techno-economic assessment, there are still many studies that employ annual-average assumptions and fail to fully capture the dynamic interaction between reliability, use of storage and curtailment [15]. More generally, PV sizing, storage and cost are frequently examined in isolation and not in one physically consistent hourly time scale [16]. Accordingly, there is a crucial gap which is the lack of studies that incorporate the combination of 8760 hours of simulation, explicit reliability assessment, physically consistent energy-power modeling of the battery, enforceable SOC limits, quantified PV curtailment, and integrated cost-reliability trade-off analyses in a single transparent off-grid desalination

framework. This gap provides a motivation for the present work.

3. Methodology

This work takes a fully simulation-based developing, evaluating and optimizing an off-grid solar powered desalination system for remote communities. All the components are dynamically modeled in the form of physical models in the MATLAB tool at hourly time resolution over 8760 h, with an emphasis on physical consistency, transparency, and reproducibility. The overall workflow with part of the component interactions, dispatch logic, and performance evaluation is summarized in Figure 1.

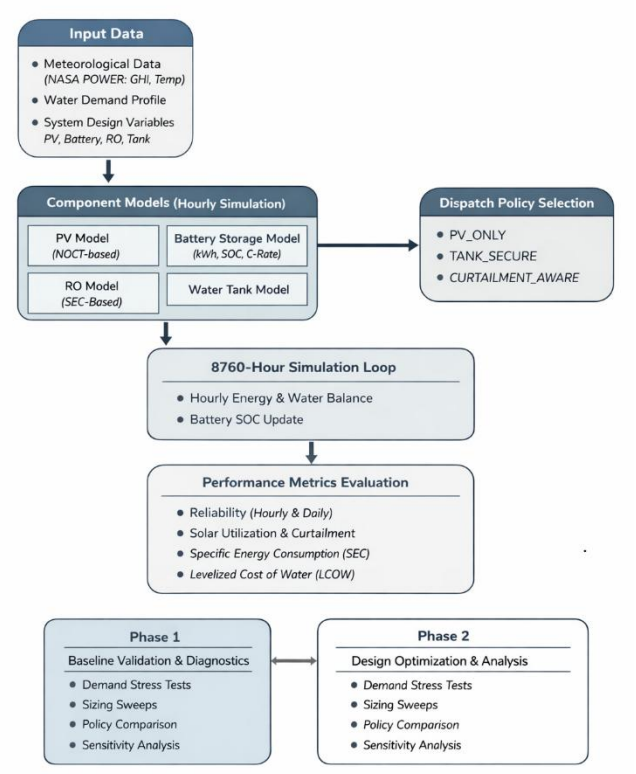

Figure 1. Overall simulation workflow of the PV–battery–RO–tank desalination system, illustrating component interactions, rule-based dispatch logic, hourly performance evaluation, and System configuration

The proposed desalination system consists of four directly coupled subsystems in off-grid configuration, i.e. (i) photovoltaic (PV) array, (ii) battery energy storage, (iii) reverse osmosis (RO) desalination unit, and (iv) freshwater storage tank. The PV array in turn drives DC power to a central electrical bus in which energy is dynamically fed to the RO operation, battery charge or curtailment in instances where the generation is higher than the immediate demand and storage capacity. Depending on the dispatch policy the battery is capable of discharging to support the operation of the RO during non-solar hours. The water tank provides short-term and diurnal buffering of freshwater production to the demands of the community. The system is modelled as PV-primary fully autonomous with no grid connection & no diesel generator.

3.1 Meteorological data

Hourly meteorological inputs are necessary to reflect the variability with time of solar-powered desalination systems and evaluate reliability under the real conditions of operation. In this study, Global Horizontal Irradiance (GHI) and ambient air temperature data were acquired on an hourly basis from the NASA POWER Project through Data Access Viewer for 1 full annual cycle. For the Phase 2 analysis, the dataset is for 1 September 2024 to 31 August 2025 for a site at 30.7264, 76.7684 for location-specific performance evaluation. This data becomes the cornerstone of the simulation framework of 8760 h simulation. GHI and ambient temperature were directly used in PV model. Missing values have been treated by linear interpolation, and nearest end extrapolation on the boundaries, negative values of irradiance was clipped to zero and ambient temperature was bounded within a physically reasonable range to ensure numerical stability and realism [17]. Because only one full annual meteorological realization was used, the levels of interannual variability were not considered, and the multi-year validation is future work.

3.2 Component models

All the system components are modelled based on system-level formulations consistent with published literature and suitable for long-term/ hourly simulations. The models have priority of physical interpretability, and at the same time, ensure computational efficiency.

PV model: The PV array was modeled with a rated power formulation that included temperature correction that relied on the Nominal Operating Cell Temperature (NOCT) method that was included in the simulation code. For each hourly time step, the cell temperature was estimated first using Eq. (1):

$$T_c = T_{amb} + \frac{NOCT-20}{800} G \quad (1)$$

where T_c is the PV cell temperature (°C), $T_{amb}$is the ambient temperature (°C), and $G$is the incident irradiance (W/ m^2). The hourly DC power output of the PV array was then calculated using Eq. (2):

$$P_{PV,dc} = P_{rated}\left(\frac{G}{G_{STC}}\right)[1+\gamma(T_c-25)] \quad (2)$$

where $P_{rated}$is the rated PV capacity, $G_{STC}$is the irradiance at standard test conditions, and $\gamma$is the linear temperature coefficient. The DC-bus power available to the desalination system was then obtained using Eq. (3):

$$P_{PV,bus} = \eta_{bus} P_{PV,dc} \quad (3)$$

Accordingly, the "total accessible PV energy" in this study is the PV energy accumulated at the DC bus after the application of Eq. (3) and not the theoretical resource based on irradiance before electrical losses. In this study, a constant aggregate DC bus efficiency was used to represent inverter, controller and wiring losses as a first order system level approximation. Although the model uses parameters representative of commercially mature crystalline-silicon modules, an additional sensitivity analysis was done using alternative representative PV parameter sets to examine the influence of different PV technology characteristics on system performance.

Battery model: The battery energy storage system was modeled in order to achieve physical consistency and to make a clear distinction between energy capacity and power capability. Battery capacity was defined as being in kWh, while the usable energy window was defined based on the allowable SOC range by using Eq. (4):

$$E_{usable} = E_{bat}(SOC_{max} - SOC_{min}) \quad (4)$$

In order to prevent unrealistically large power exchange by small-capacity batteries, the maximum charging and discharging powers were related to battery capacity by the selected C-rate as given in Eqs.: (5) and (6):

$$P_{ch,max} = C_{rate}E_{bat} \quad (5)$$

$$P_{dis,max} = C_{rate}E_{bat} \quad (6)$$

The hourly SOC update was then calculated from the charge-discharge energy balance using Eq. (7):

$$SOC_{k+1} = SOC_k + \frac{\eta_{ch}P_{ch}\Delta t - P_{dis}\Delta t/\eta_{dis}}{E_{bat}} \quad (7)$$

When E_{bat}=0, all the dynamics of SOC, charge/discharge limits, and effects of battery efficiency were switched off automatically, and the system worked in PV-direct configuration without electrical storage. Battery aging was not considered in the baseline model as its effect was assessed separately in a bounding sensitivity analysis.

RO model: A specific-energy-consumption (SEC)-based model was used to formulate the reverse-osmosis (RO) unit giving the direct connection between electrical input and the freshwater production on a per-hour basis. The total electrical power needed for the RO unit was determined by the Eq. (8):

$$P_{RO} = P_{aux} + SEC \cdot Q_{RO} \quad (8)$$

where P_{aux} is the fixed auxiliary load due to pretreatment, pumping and control systems and is the hourly freshwater production rate. Accordingly, hourly RO production was calculated from the net power available to membranes using Eq. (9).

$$Q_{RO} = \frac{P_{RO,net} - P_{aux}}{SEC} \quad (9)$$

Subject to maximum RO production capacity and available tank headroom; Partial load operation was allowed when available power was too little for rated production. The baseline model assumes constant SEC as tractable system level approximation; the effects of part load inefficiency and membrane ageing were however evaluated separately through bounding sensitivity analysis.

Water tank model: The water tank was modelled as an hourly storage buffer for fresh water that connects the RO production with community water supply. At each hourly time step, storage in the tank was updated from the balance between RO inflow and community withdrawal, while making sure the volume stored in the tank was kept within the available tank storage volume. The post-demand tank volume dictated the amount of water that could be supplied and the amount of headroom available for RO production in the same hour. Two operational thresholds were defined in order to make dispatch decisions: a secure volume and a target volume. These were expressed quantitatively as fixed fractions of tank capacity, namely

$$V_{secure} = 0.30\,V_{max} \quad (10)$$

and

$$V_{target} = 0.70\,V_{max} \quad (11)$$

where V_{max} is the total capacity of tanks as used in the control logic, the secure volume is the minimum strategic buffer (short term water reliability) volume, while the target volume is the preferred level of operation (storage recovery). These thresholds give the water tank the role of strategic buffer, and reduce the need for unnecessary dependence on the battery storage by affecting when RO production is prioritized.

Dispatch policies: Three rule-based dispatch policies under identical climatic and system conditions were implemented and evaluated. PV only In PV only the RO unit works when the instantaneous PV is sufficient and does not discharge the battery. In TANK_SECURE, for post-demand tank RO operation is favored if the post-demand tank volume is lower than the target volume cap, and battery support will be permitted only if the tank volume is lower than the secure volume cap, to help restore minimum water security. In Case of CURTAILMENT_AWARE, the above logic is further extended to support opportunistic RO operation in the surplus PV generation, which would otherwise be curtailed, hence improve the solar energy utilization. Algorithmically, dispatch evaluates the status of tank in relation to V_secureand V_target followed by the decision to perform RO operation and then the decision to admissible battery support under selected policy.

Performance metrics: System performance was assessed with the complementary indicators of reliability, energy and economic performance. Hourly reliability was defined as the ratio between the volume of simulated hours that had zero unmet water demand, as provided in Eq. (12):

$$R_{hourly} = \frac{N(U_h=0)}{N_h} \quad (12)$$

where $U_h$is the hourly unmet demand, $N(U_h = 0)$is the number of hours with no unmet demand, and $N_h$is the total number of simulated hours. Daily reliability was defined as the fraction of days for which the full daily water demand was satisfied, as shown in Eq. (13):

$$R_{daily} = \frac{N(U_d=0)}{N_d} \quad (13)$$

where $U_d$is the total unmet demand over a day and $N_d$is the number of simulated days. In addition, unmet demand was quantified using annual unmet volume, unmet-demand percentage, shortage days, and average shortage per failure day.

Solar utilization was defined as the ratio of accessible PV energy at the DC bus in actual use for RO operation or battery charging and given by Eq. (14):

$$SU = \frac{E_{PV,used}}{E_{PV,bus}} \quad (14)$$

The curtailment fraction was calculated using Eq. (15):

$$CF = \frac{E_{curt}}{E_{PV,bus}} \quad (15)$$

where $E_{PV,bus}$ is the total PV energy available at the DC bus and E_{curt} is the curtailed PV energy. The realized specific energy consumption (SEC) was computed from Eq. (16):

$$SEC_{real} = \frac{E_{RO}}{W_{prod}} \quad (16)$$

where E_{RO} is the total electrical energy supplied to the RO unit and W_{prod} is the total freshwater produced.

Economic performance was assessed using the levelized cost of water (LCOW), defined in Eq. (17) as:

$$LCOW = \frac{CRF \cdot CAPEX + OPEX_{annual}}{W_{delivered}} \quad (17)$$

where $CAPEX$ includes the costs of PV capacity, battery energy capacity, RO production capacity, and tank volume; $OPEX_{annual}$ is the annual operating cost; $W_{delivered}$ is the annual delivered freshwater volume; and CRF is the capital recovery factor. In the present study, $OPEX_{annual}$ was assumed to be 4% of $CAPEX$, the discount rate was taken as 8%, and the project lifetime was assumed to be 20 years also shown in Table 1. Replacement costs were not included directly in the baseline LCOW formulation; instead, the possible effects of battery aging and membrane-related replacement were evaluated separately through bounding sensitivity analyses.

Table 1. Economic assumptions used in LCOW calculation

Parameter	Value
PV cost	1000 USD/kW
Battery cost	250 USD/kWh
RO cost	1500 USD/(m³/day)
Tank cost	120 USD/m³
Annual OPEX	4% of CAPEX
Discount rate	8%
Project lifetime	20 years

3.3 Phase structure and design-space exploration

The methodological framework was separated into two phases. Phase 1 was focused on model verification and baseline evaluation through hourly energy balance (diagnostics), water balance, SOC limit enforcement, tank capacity enforcement, as well as battery C-rate consistency checks to insure physically consistent behavior. Baseline outputs such as realized SEC, solar utilization, curtailment fraction and reliability, were also compared with literature values. Phase 2 has extended the work to systematic design space exploration where the PV capacity, battery energy capacity, RO production capacity and tank volume were varied over a discrete grid and each configuration was simulated over 8760 hours. In this enumerative co-design sweep, the feasible designs were found by applying a threshold of daily-reliability, following which trade-offs between LCOW, reliability, and solar utilization were investigated with the help of Pareto analysis.

4. Results

This section presents the annual 8760 h results of the simulations in the MATLAB environment of the PV-battery-RO-water-tank system. Phase 1 is an evaluation of baseline behavior and physical consistency, and Phase 2 is an evaluation of demand sensitivity, design space exploration, dispatch performance, and robustness for autonomous PV-primary off-grid operation.

4.1 Phase 1: Baseline system behavior

Phase 1 testing of system functionality at a nominal community water demand of 10 m³/day or equating to a yearly demand of 3650 m³. It aims at checking internal model consistency, characterizing the dynamic behavior of the coupled system of PV-battery-RO-tank and providing a quantitative basis to be used in future optimization. The revised annual water balance indicates that the system has 3643.73 m³/year desalinated water production and 3638.36 m3/year supplying, and it is 11.64 m³/year (0.319%) undistributed annually. Accordingly, the baseline case results in 98.63% daily reliability, with 5 days/year of shortage and 2.33 m³ per failure day average shortage, instead of 100% uninterrupted service. Figure 2 shows the hourly distribution of PV power during a representative week: PV is to support first the RO operation and then battery charging and the remaining surplus is curtailed. During the year, the PV bus delivers 32,437 kWh which resulted in 56.43% solar utilization and 43.57% curtailment. Actual SEC is 4.74 kWh/m³ and the final tank storage is 20.37 m³, which proves that there is stable but not lossless operation.

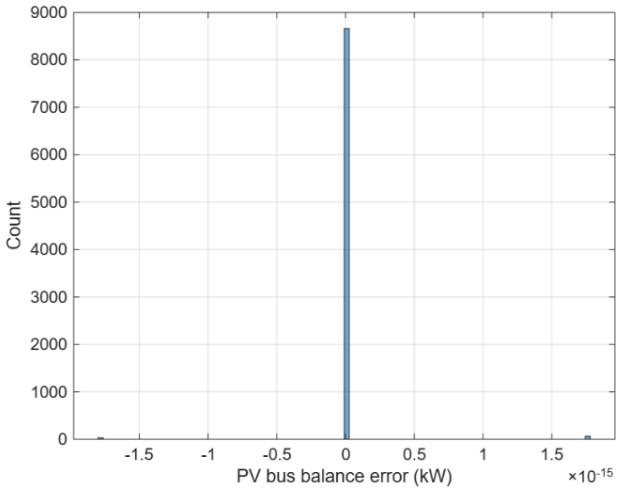

Figure 2. Hourly photovoltaic power allocation during a representative week of baseline operation, showing the distribution of PV energy to RO operation, battery charging, and curtailment

The dynamics of water tanks are illustrated in Figure 3. The tank has a predictable diurnal cycling with the storage increasing during the day as RO operation is on and decreasing when withdrawal periods occur as community demand is met. However, the revised results for the annual period are based on the conclusion that tank volume is not always kept above the secure threshold all year round. Instead, the base case has a large, but imperfect level of buffering performance with 5 shortage days and an annual unmet demand of 11.64 m³. The seasonal analysis goes on to show that these shortfalls are clustered in the month of May which suggests that reliability loss is linked to temporally concentrated operational stress rather than persistent tank inadequacy. Even so, the tank is an effective short-term storage buffer and the final tank storage of 20.37 m³ provides evidence of significant residual storage throughout most of the year.

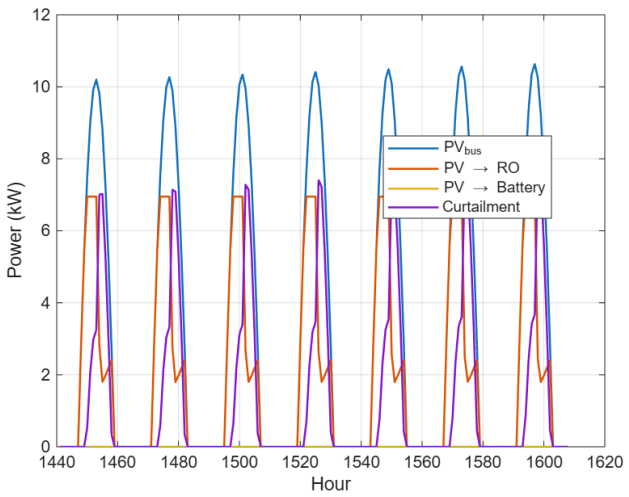

Figure 3. Temporal evolution of freshwater tank volume during a representative week under baseline conditions

A plot of the hourly production profile of RO water is presented in Figure 4. The production of fresh water is strongly related to the availability of solar energy and partial-load operation is realized in periods of moderate irradiance when full RO power is not available. In the revised baseline results, the total annual energy contributed to the RO unit comes to about 17,281 kWh which renders the SEC to 4.74 kWh/m3 realized. This value is still within the range that is typically reported for small scale RO systems and validates the physical consistency of the baseline simulation.

Battery state-of-charge (SOC) behavior is shown in Figure 5. The SOC is found to mostly be near the upper limit, with only shallow discharges occurring for low irradiance hours. This trend is in line with the diagnostics of the baseline, which indicate a limited battery cycling and justifies the interpretation that the battery is mainly a short-term balancing buffer but not a comprehensively cycled storage resource. This result is also helpful in understanding the subsequent design space trends, where a portion of the reliability function can be shifted between electrical storage and water storage.

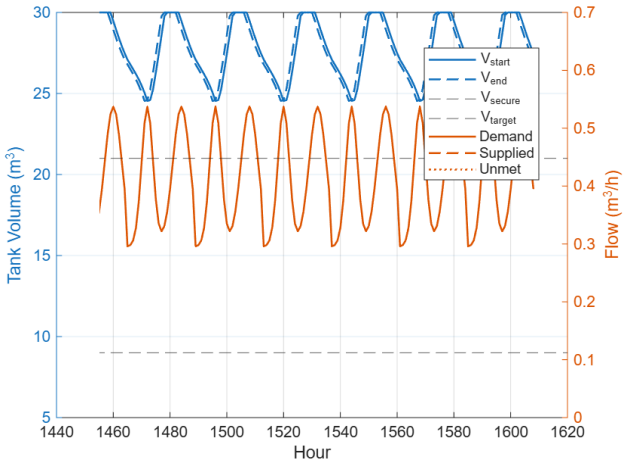

Figure 4. Hourly reverse osmosis water production profile during a representative week of baseline operation

Errors in PV energy balance over one hour is not on the order of 10-15 kW, instead the revised PV - bus energy balance diagnostic confirms a numerical exact accounting over an entire hour with a maximum absolute balance error of only 1.78 x 10-15 kW, proving a very high level of numerical consistency. Table 2 shows an overview of the baseline annual performance metrics.

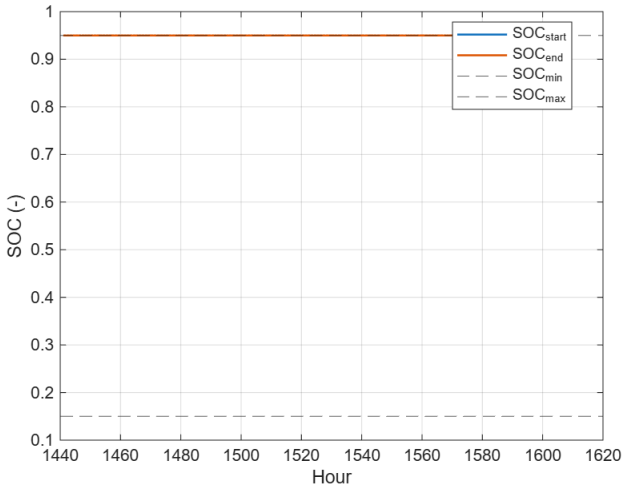

Figure 5. Battery state-of-charge profile highlighting limited cycling behavior under baseline conditions

Table 2. Phase-1 baseline annual performance metrics (10 m^3/day demand)

Metric	Value
Annual water demand	3650 m^3
Annual RO water produced	3643.73 m^3
Annual water supplied	3638.36 m^3
Annual unmet demand	11.64 m3 (0.319%)
Daily reliability	98.63%
PV bus energy available	32,437 kWh
Solar utilization	56.43%
PV energy curtailed	43.57%
Realized SEC	4.74 kWh/m^3
Shortage days	5 days/year
Average shortage per failure day	2.33 m^3/day
Final tank storage	20.37 m^3

4.2 Phase 2A: Demand sensitivity

Phase 2A studies the systems performance at community water demands (based on 5, 10, 15 and 20 m^3/day) operating under three dispatch policies (PV_ONLY, TANK_SECURE and CURTAILMENT_AWARE). Figure 6 shows the variation with demand of the daily reliability and LCOW. At a flow rate of 5 m^3/day all the policies have 100% daily reliability and zero unmet demand. However, as the demand grows, there is a strong break in reliability for PV_ONLY: for 15 m^3/day, reliability is 27.67% with 13.77% unmet demand and for 20 m3/day reliability is 0.55% with 35.05% unmet demand, since it is only dependent on PV (instantaneous) availability. In comparison, TANK_SECURE and CURTAILMENT_AWARE

have much higher reliability (98.36-98.63%) for 10 m^3/day, about 85.48% for 15 m^3/day and 41.64% for 20 m^3/day. Under CURTAILMENT_AWARE, LCOW goes from 6.81 to 2.02 USD/m^3 as demand increases and solar utilization increases to 95.34% and curtailment goes down to 4.66% (Table 3).

4.3 Phase 2B: Design-space exploration

The coupled design space of PV capacity, battery energy capacity, RO production capacity, and tank volume are investigated in Phase 2B. Feasible designs are considered to be those with daily reliability of at least 95%. Solar utilization as a function of PV size for feasible configurations is shown in Figure 7 together with the corresponding Pareto front between LCOW and solar utilization. Larger PV capacity generally makes the feasibility better, but it also has diminishing returns in the utilization of unless accompanied by sufficient battery, tank or RO capacity. The outcomes of the revised design-space results confirm that the feasible region has several Pareto-efficient solutions instead of one global optimum enabling flexibility of adaptation to site-specific circumstances. A recommended knee point design was also found among the Pareto set. Representative feasible configurations are summarized in Table 4.

Compares the baseline and minimum-LCOW feasible designs which highlights the cost-reliability tradeoff between economic efficiency and service performance presented in Table 5.

4.4 Phase 2C: Heatmap analysis

A heatmap of the daily reliability as a function of battery capacity and tank volume is presented in Figure 8 for the representative case of PV = 20 kW, RO = 1.5 m^3/h and demand = 10 m^3/day. Reliability indicates that there is a strong initial improvement with the inclusion of storage, which then reduces with moderate storage sizes. For instance, increases in battery capacity range from 0 to 20 kWh led to significant improvements of reliability for all tank sizes, whereas for 40 - 60 kWh, there are smaller gains. A similar trend can be seen for tank volume. Importantly, larger tank volumes can compensate to some extent for the lower battery capacity: e.g. the reliability rises from ca. 0.93 at 0 kWh and 10 m3 to ca. 0.98 at 0 kWh and 40 m^3. The outcome of this experiment demonstrates the importance of water storage as strategic reliability buffer and validates the fact that battery storage and tank storage are partially replaceable in remote desalination design.

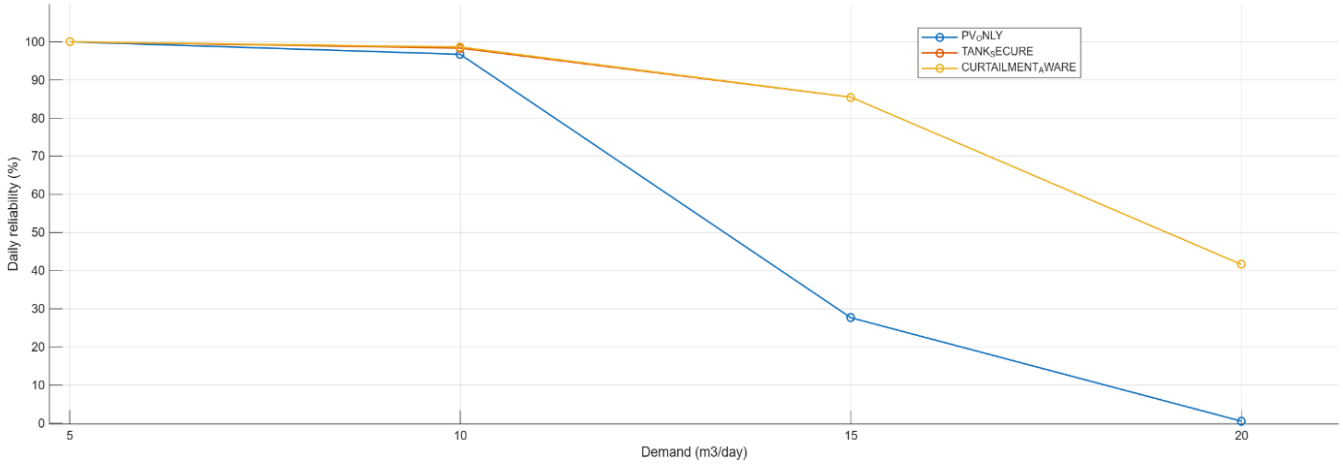

Figure 6. Daily reliability and levelized cost of water as functions of community water demand for different dispatch policies

Table 3. Phase-2A demand sensitivity results

Policy	Demand (m3/day)	Daily reliability (%)	Unmet demand (%)	Solar utilization (%)	Curtailment (%)	LCOW (USD/m^3)
PV_ONLY	5	100.00	0.00	28.19	71.81	6.81
PV_ONLY	10	96.71	0.91	55.31	44.69	3.44
PV_ONLY	15	27.67	13.77	71.98	28.02	2.63
PV_ONLY	20	0.55	35.05	72.29	27.71	2.62
TANK_SECURE	5	100.00	0.00	28.19	71.81	6.81
TANK_SECURE	10	98.36	0.42	55.62	44.38	3.42
TANK_SECURE	15	85.48	3.69	81.02	18.98	2.36
TANK_SECURE	20	41.64	15.83	95.34	4.66	2.02
CURTAILMENT_AWARE	5	100.00	0.00	29.86	70.14	6.81
CURTAILMENT_AWARE	10	98.63	0.32	56.43	43.57	3.42
CURTAILMENT_AWARE	15	85.48	3.68	81.03	18.97	2.36
CURTAILMENT_AWARE	20	41.64	15.83	95.34	4.66	2.02

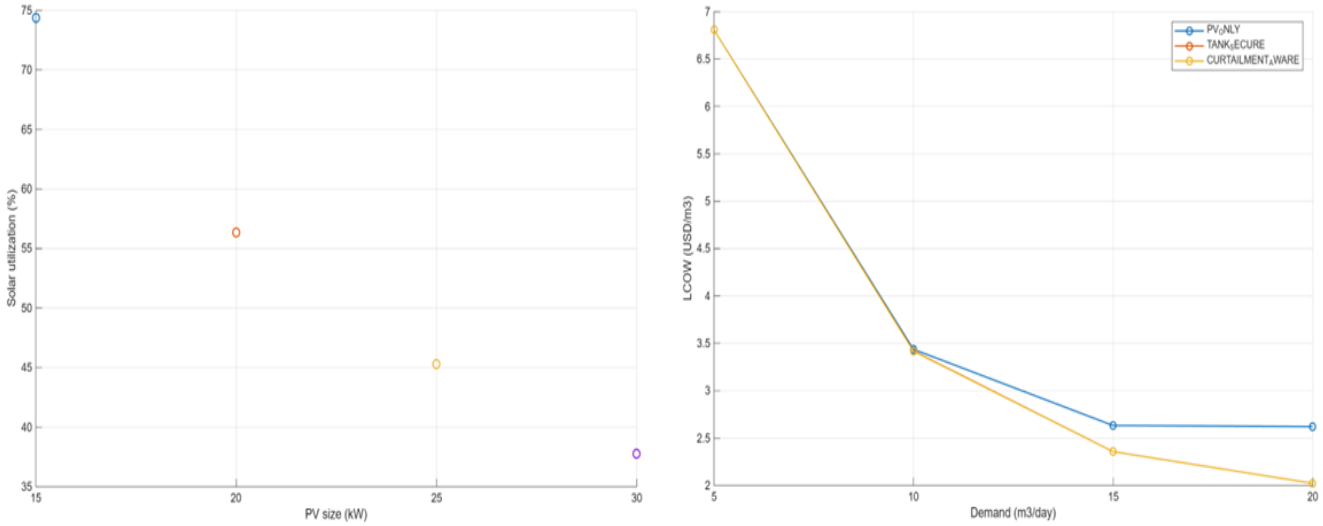

Figure 7. Design-space exploration results showing solar utilization versus PV size and the Pareto front between LCOW and solar utilization for feasible designs

Table 4. Representative feasible designs meeting ≥95% reliability

Design category	PV (kW)	Battery (kWh)	Tank (m^3)	RO (m^3/h)	Daily reliability (%)	Solar utilization (%)	Curtailment (%)	LCOW (USD/m^3)
Minimum-LCOW feasible design	20	20	40	0.8	95.07	57.18	42.82	2.31
Balanced feasible design	20	40	20	0.8	96.99	57.51	42.49	2.40
High-utilization feasible design	15	20	40	1.5	95.62	74.44	25.56	3.11

Table 5. Baseline versus optimized feasible system design comparison

Metric	Baseline design	Optimized feasible design	Change
PV capacity (kW)	20.00	20.00	0.00%
Battery capacity (kWh)	40.00	20.00	-50.00%
Tank capacity (m3)	30.00	40.00	+33.33%
RO capacity (m3/h)	1.50	0.80	-46.67%
Annual water production (m3)	3643.73	3593.08	-1.39%
Annual water demand (m3)	3650.00	3650.00	0.00%
Annual unmet water (m3)	11.64	46.76	+301.86%
Unmet demand (%)	0.319	1.281	+301.86%
Daily reliability (%)	98.63	95.07	-3.61%
Solar utilization (%)	56.43	57.18	+1.33%
Curtailment (%)	43.57	42.82	-1.72%
LCOW (USD/m3)	3.415	2.307	-32.45%
Shortage days (days/year)	5	18	+260.00%
Average shortage per failure day (m3/day)	2.33	2.60	+11.55%
Excess water (m3/year)	-6.27	-56.92	-808.03%
Final tank storage (m3)	20.37	24.95	+22.47%

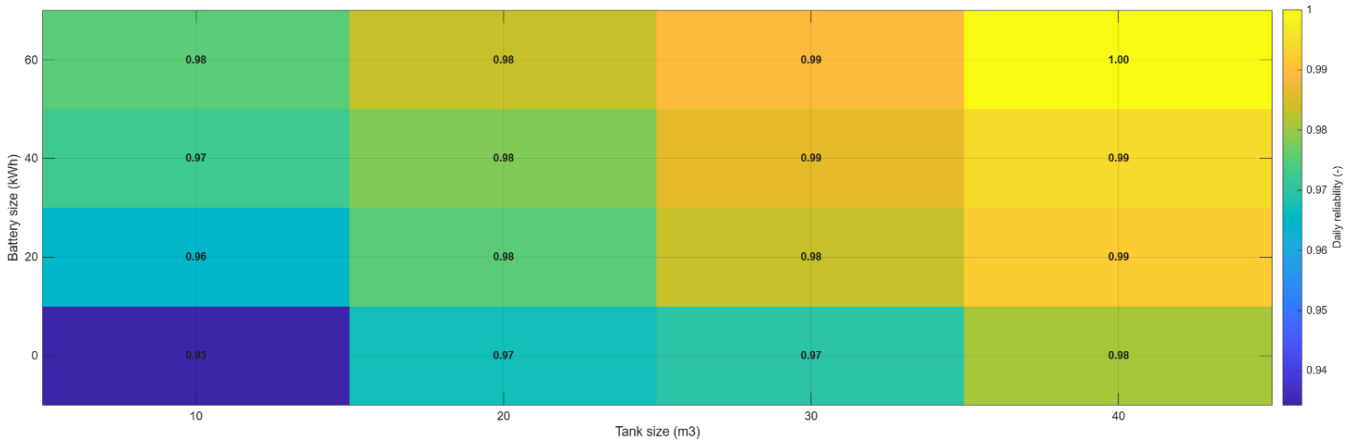

Figure 8. Daily reliability heatmap as a function of battery energy capacity and freshwater tank volume

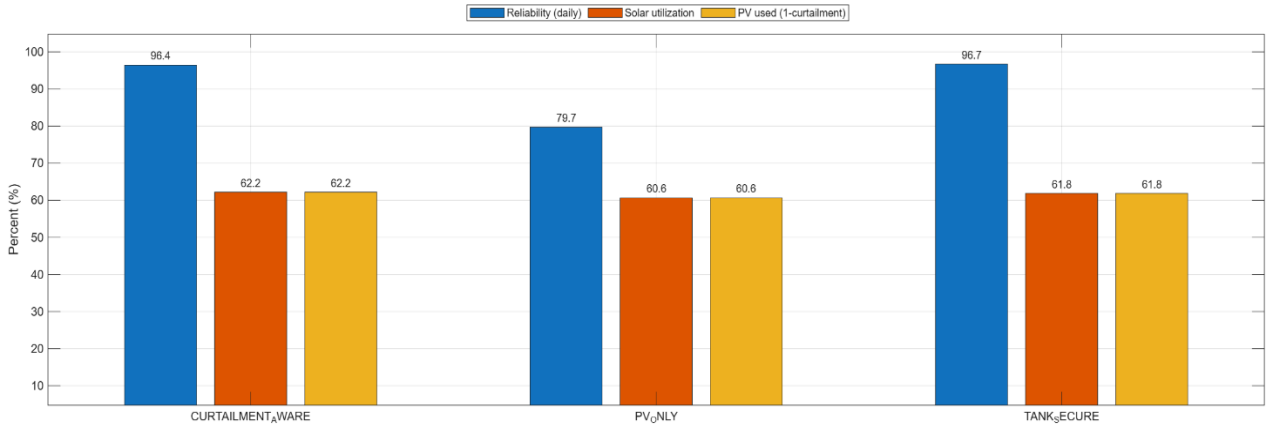

Figure 9. Comparison of dispatch policies in terms of daily reliability, solar utilization, and levelized cost of water

Table 6. Phase-2D policy-level performance comparison (10 m^3/day)

Policy	Daily reliability (%)	Unmet demand (%)	Solar utilization (%)	Curtailment (%)	LCOW (USD/m^3)
PV_ONLY	96.71	0.91	55.31	44.69	3.44
TANK_SECURE	98.36	0.42	55.62	44.38	3.42
CURTAILMENT_AWARE	98.63	0.32	56.43	43.57	3.42

4.5 Phase 2D: Policy comparison

Dispatch policies are compared with the help of bar charts of reliability, solar utilization and LCOW in Figure 9. The policy, which has the name of CURTAILMENT_AWARE, is always more efficient to maximize the solar utilization while maintaining equal or better reliability than TANK_SECURE. The PV_ONLY policy has the worst performance according to all aspects. Table 6 summarizes performance at the policy level.

4.6 Phase 2E: Sensitivity analysis

Figure 10 presents a tornado plot of the sensitivity of LCOW to the main parameters. Community demand is the primary cost driver followed by RO SEC, whereas battery efficiency has little impact for the range tested. A 25% drop in demand gives a 32.91% increase in LCOW, but a 25% increase gives a 18.96% decrease. By comparison, varying SEC by +-20% causes a change in LCOW of only -0.32% to +0.69%, and lowering battery efficiency from 0.95 to 0.90 causes a change in LCOW of only 0.01%. Bounding analyses further reveal that severe battery aging results in LCOW increasing to about 3.490 USD/m^3 and severe membrane aging and 20% part-load SEC penalty results in LCOW increasing to about 3.655 and 3.439 USD/m^3, respectively, with only minor reductions in reliability. The results of LCOW and reliability are summarized in Table 7. To quantify the probable impacts of non-ideal component behavior beyond the baseline model, additional bounding cases were considered for battery aging, membrane aging and part load RO inefficiency. The resulting impacts on reliability, unmet demand and LCOW are summarised in Table 8.

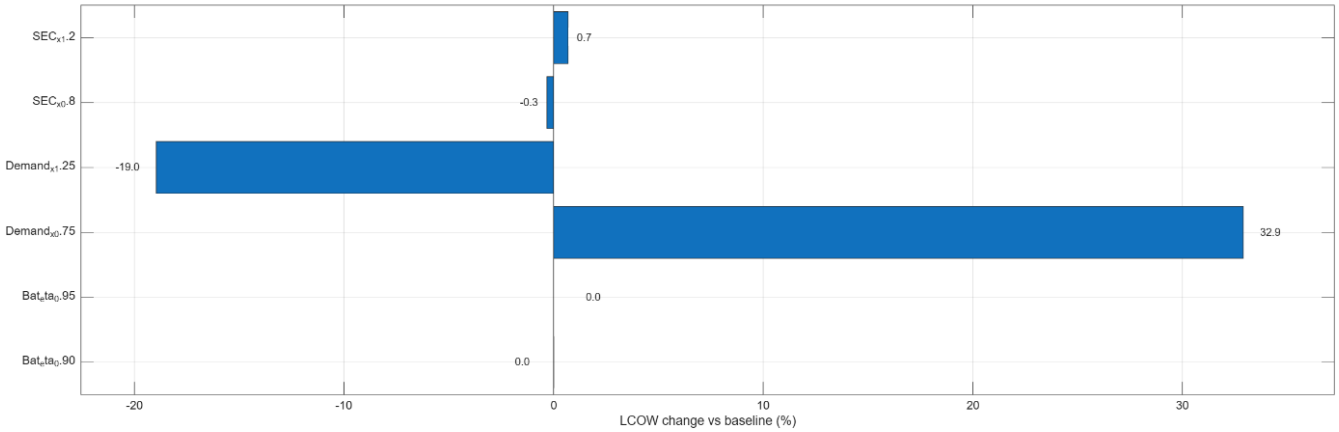

Figure 10. Tornado plot showing sensitivity of levelized cost of water to key system parameters

Table 7. Phase-2E sensitivity results for LCOW and reliability

Case	LCOW (USD/m³)	LCOW change (%)	Daily reliability (%)
SEC x 0.8	3.4045	-0.32	100.00
SEC x 1.2	3.4390	0.69	96.99
Demand x 0.75	4.5393	32.91	100.00
Demand x 1.25	2.7679	-18.96	95.07
Battery eta = 0.95	3.4153	0.00	98.63
Battery eta = 0.90	3.4157	0.01	98.63

Table 8. Bounding sensitivity results for degradation-related scenarios

Scenario	Daily reliability (%)	Unmet demand (%)	LCOW (USD/m³)
Baseline	98.63	0.319	3.415
Severe battery aging	98.36	0.362	3.490
Severe membrane aging	97.26	0.840	3.655
20% part-load SEC penalty	96.99	1.006	3.439

Overall, the results indicate that high levels of reliability are not sufficient for efficient off-grid desalination. It can be stressed that coordinated system sizing and curtailment aware dispatch can be used to reduce PV curtailment, reduce water cost and provide sustainable freshwater solution to remote communities.

5. Discussion

The outcomes of this study give a system level insight into the design of off-grid solar-powered desalination systems to meet the balance of reliability, efficiency and cost under the operational constraints characteristic of remote communities. The analysis transcends the use of either a static or averaged framework of PV generation, battery storage, RO desalination, and freshwater storage, and reflects the dynamism of interactions between the theoretically feasible and economically viable design and operations of a particular design by employing an hourly resolved (8760 h) framework of physical consistent models. One of the key conclusions is that it is often economically inefficient to make the off-grid solar-powered desalination systems 100% reliable. While near perfect reliability can certainly be achieved in theory, high PV oversizing, high curtailment, and underutilization of installed assets can be necessary to achieve near perfect reliability. The phase 2 demonstrates that slightly less strict reliability thresholds, including requiring that of 95 percent daily reliability, can become large treats in solar uptake and in LCOW reduction. For remote communities, however, such service levels may be acceptable particularly were complemented by short-term water storage or demand side flexibility.

The study also clarifies the role played by storage. Even though batteries are frequently considered the primary reaction to the variability of the solar power, the base level performance demonstrates insignificant cycling and a flat SOC profile, which means that a battery is presented as a short-term balancing buffer rather than a deep-shifting energy source. In the design space exploration, the reliability increases reduce with battery capacity exceeding the moderate levels, and the capital cost rises. In contrast, freshwater storage has been identified as an important and low-cost reliability buffer. The results of the heatmap and feasible design indicate that one can partially replace the battery capacity by increasing the volume of the tank. This is particularly relevant to remote applications where water tanks are easier to fabricate, install and maintain than electrochemical storage systems. Photovoltaic curtailment is another understanding. Rather than just seen as a bad thing, high curtailment should be taken as an indication of mismatch between PV capacity, RO throughput, storage and dispatch strategy. The good performance of the curtailment-aware policy indicates that dispatch logic is an additional design variable, in addition to component sizing. Comparing with the existing studies, the numerical performance of the proposed system is in the general agreement with the values found in the literature for small-scale PV-powered RO desalination.

Reported specific energy consumption values are within the ranges reported by [18,19], LCOW values are within the ranges reported by [20,21] for off-grid and for hybrid renewable desalination systems, respectively However, many previous works implicitly assume reliability, often averaged energy balances are used, or explicit accounting of PV curtailment is not performed. References [22,23] indicate the need of hybrid storage and control, but often explicit quantification of the interaction among reliability, curtailment, and cost is not performed on the hourly time scale. The present study goes beyond state of the art by explicitly testing reliability at the hourly and daily level, physically enforcing the consistency between battery energy and power by using C-rate constraints, and by using curtailment as a central performance measure and not a residual outcome.

For practical design and fabrication, the findings provide three major insights: it is not a good idea to adopt large battery systems by default, but balanced investment is required in the areas of PV capacity, RO throughput, electrical storage, and water storage; oversizing PV without corresponding conversion and storage capacity mainly results in increased curtailment rather than service quality; the application of simple rule-based dispatch can significantly improve efficiency and cost, making control strategy especially valuable for use in areas with low complexity remote community deployments. The research has a number of limitations. It is based on hourly climate data from one location and one representative annual realization only, therefore, interannual variability, extreme events and true multi-year robustness could not be assessed and meaningful year-to-year uncertainty statistics are outside the scope of the available dataset. The RO subsystem was modeled with a constant SEC formulation, so that the effects of salinity, temperature, membrane aging and part load effects were not explicitly modeled. The PV performance degradation and battery aging are components degradation which were not part of the baseline model. In addition, fixed unit cost assumptions were adopted and LCOW should be taken as a comparative design indicator rather than a site-specific financial prediction. The framework should be expanded in future work to involve multi-year simulations in various climatic areas and add element degradation, which will enable the evaluation of interannual robustness, uncertainty in reliability and LCOW, as well as replacement planning to be evaluated more rigorously. Additional gains also may be realized by adaptive or predictive dispatch strategies such as model predictive control to improve reliability, utilization, and cost under uncertain operating conditions.

6. Conclusion

This research suggested a physically consistent simulation framework for design and analysis of an off-grid solar powered desalination system for remote communities. Using an hourly resolved 8760 h model in the Matlab programming language that integrates photovoltaic generation, battery storage, reverse osmosis desalination and freshwater storage, the results revealed that it is possible to achieve high service reliability without having to rely on grid electricity nor on fossil-fuel backup. However, the analysis also revealed that maximising reliability is not always economically efficient. The baseline case showed a high 98.63% reliability at the daily level with a low 0.319% unmet demand but a high amount of PV curtailment. Design-space exploration showed that a minimum-LCOW feasible design can result in a reduction of up to 32.45% in water cost; however, with a degree of reduction of reliability. The results have further found that battery storage is not always the most cost-effective reliability buffer. Water storage can partially replace the battery capacity and curtailment-aware dispatch can enhance the utilization rate of the solar power while ensuring a high reliability. Sensitivity analyses verified that community demand is the primary LCOW driver with an insignificant contribution from battery efficiency; while another set of bounding cases indicated that battery aging, membrane aging, and part load SEC penalties affect the results in quantifiable but small amounts. Although limited to one climatic location as well as a simplified SEC-based RO representation, the study offers a useful design basis for future multi-year and degradation-aware and regionally comparative analyses.

Ethical issue

The authors are aware of and comply with best practices in publication ethics, specifically with regard to authorship (avoidance of guest authorship), dual submission, manipulation of figures, competing interests, and compliance with policies on research ethics. The authors adhere to publication requirements that the submitted work is original and has not been published elsewhere. All survey participants provided informed consent prior to participation, and the anonymity and confidentiality of all respondents were strictly maintained throughout the research process.

Data availability statement

The manuscript contains all the data. However, additional data will be provided by the corresponding author upon reasonable request.

Conflict of interest

The authors declare no potential conflict of interest.

References

[1] M. A. Dawoud, G. R. Sallam, M. A. Abdelrahman, and M. Emam, “The performance and feasibility of solar-powered desalination for brackish groundwater in Egypt,” Sustainability, vol. 16, no. 4, p. 1630, 2024.

[2] S. Alqaed, J. Mustafa, and F. A. Almehmadi, “Design and energy requirements of a photovoltaic-thermal powered water desalination plant for the Middle East,” Int. J. Environ. Res. Public Health, vol. 18, no. 3, p. 1001, 2021.

[3] V. Powar and R. Singh, “Stand-alone direct current power network based on photovoltaics and lithium-ion batteries for reverse osmosis desalination plant,” Energies, vol. 14, no. 10, p. 2772, 2021.

[4] M. Najaftomaraei, M. Osouli, H. Erbay, M. H. Shahverdian, A. Sohani, K. Mazarei Saadabadi, and H. Sayyaadi, “Artificial intelligence-based optimization of renewable-powered RO desalination for reduced grid dependence,” Water, vol. 17, no. 13, p. 1981, 2025.

[5] K. Menon, M. Jia, S. Kaur, C. Dames, and R. S. Prasher, “Distributed desalination using solar energy: A technoeconomic framework to decarbonize

nontraditional water treatment," iScience, vol. 26, no. 2, 2023.
[6] Z. A. Haidar, M. Al-Saud, J. Orfi, and H. Al-Ansary, "Reverse osmosis desalination plants energy consumption management and optimization for improving power systems voltage stability with PV generation resources," Energies, vol. 14, no. 22, p. 7739, 2021.
[7] M. A. Al-Obaidi, S. Alsadaie, A. Alsarayreh, M. T. Sowgath, and I. M. Mujtaba, "Integration of renewable energy systems in desalination," Processes, vol. 12, no. 4, p. 770, 2024.
[8] M. M. Armendáriz-Ontiveros, G. E. Dévora-Isiordia, J. Rodríguez-López, R. G. Sánchez-Duarte, J. Álvarez-Sánchez, Y. Villegas-Peralta, and M. D. R. Martínez-Macias, "Effect of temperature on energy consumption and polarization in reverse osmosis desalination using a spray-cooled photovoltaic system," Energies, vol. 15, no. 20, p. 7787, 2022.
[9] G. Azinheira, R. Segurado, and M. Costa, "Is renewable energy-powered desalination a viable solution for water stressed regions? A case study in Algarve, Portugal," Energies, vol. 12, no. 24, p. 4651, 2019.
[10] E. Ahmadi, B. McLellan, B. Mohammadi-Ivatloo, and T. Tezuka, "The role of renewable energy resources in sustainability of water desalination as a potential fresh-water source: An updated review," Sustainability, vol. 12, no. 13, p. 5233, 2020.
[11] R. S. Alshareef, B. A. Almohammadi, H. A. Refaey, M. Farhan, and M. A. Sharafeldin, "Investigation of the performance and use of a solar cell integrated with a reverse-osmosis water-desalination system," Energies, vol. 17, no. 16, p. 4010, 2024.
[12] O. Zeitoun, J. Orfi, S. U. D. Khan, and H. Al-Ansary, "Desalinated water costs from steam, combined, and nuclear cogeneration plants using power and heat allocation methods," Energies, vol. 16, no. 6, p. 2752, 2023.
[13] R. Apolinário and R. Castro, "Solar-powered desalination as a sustainable long-term solution for the water scarcity problem: Case studies in Portugal," Water, vol. 16, no. 15, p. 2140, 2024.
[14] L. Gevorkov, J. L. Domínguez-García, and L. Trilla, "The synergy of renewable energy and desalination: An overview of current practices and future directions," Applied Sciences, vol. 15, no. 4, p. 1794, 2025.
[15] E. M. Almetwally, M. A. Elazab, A. E. Kabeel, Y. Yasser, and A. Elgebaly, "Solar powered reverse osmosis desalination: A systematic review of technologies, integration strategies and challenges," Desalination, p. 119228, 2025.
[16] M. M. Mundu, J. I. Sempewo, S. N. Nnamchi, and D. E. Uti, "Solar-powered desalination technologies for sustainable water security solutions," Int. J. Energy Res., vol. 2025, no. 1, p. 3482306, 2025.
[17] NASA Langley Research Center, "Data access viewer (DAV), NASA POWER Project," 2025. [Online]. Available: https://power.larc.nasa.gov/data-access-viewer/. Accessed: Dec. 25, 2025.
[18] Z. Tigrine, H. Aburideh, D. Zioui, S. Hout, N. Sahraoui, Y. Benchoubane, et al., "Feasibility study of a reverse osmosis desalination unit powered by photovoltaic panels for a sustainable water supply in Algeria," Sustainability, vol. 15, no. 19, p. 14189, 2023.
[19] Kaya, M. E. Tok, and M. Koc, "A levelized cost analysis for solar-energy-powered sea water desalination in the Emirate of Abu Dhabi," Sustainability, vol. 11, no. 6, p. 1691, 2019.
[20] E. Cervantes-Rendón, J. Ibarra-Bahena, L. E. Cervera-Gómez, R. J. Romero, J. Cerezo, A. Rodríguez-Martínez, and U. Dehesa-Carrasco, "Rural application of a low-pressure reverse osmosis desalination system powered by solar–photovoltaic energy for Mexican arid zones," Sustainability, vol. 14, no. 17, p. 10958, 2022.
[21] M. Castro, M. Alcanzare, E. Esparcia Jr., and J. Ocon, "A comparative techno-economic analysis of different desalination technologies in off-grid islands," Energies, vol. 13, no. 9, p. 2261, 2020.
[22] L. Cornejo-Ponce, P. Vilca-Salinas, M. J. Arenas-Herrera, C. Moraga-Contreras, H. Tapia-Caroca, and S. Kukulis-Martínez, "Small-scale solar-powered desalination plants: A sustainable alternative water-energy nexus to obtain water for Chile's coastal areas," Energies, vol. 15, no. 23, p. 9245, 2022.
[23] H. M. Maghrabie, A. G. Olabi, A. Rezk, A. Radwan, A. H. Alami, and M. A. Abdelkareem, "Energy storage for water desalination systems based on renewable energy resources," Energies, vol. 16, no. 7, p. 3178, 2023.